Available online at www.sciencedirect.com
ScienceDirect
Journal of the European Ceramic Society 27 (2007) 4453–4460
www.elsevier.com/locate/jeurceramsoc

# An investigation of $(Na_{0.5}K_{0.5})NbO_3$–$CaTiO_3$ based lead-free ceramics and surface acoustic wave devices

Ren-Chuan Chang [a], Sheng-Yuan Chu [a,b,*], Yi-Fang Lin [a], Cheng-Shong Hong [a,c], Yi-Peng Wong [a]

[a] *Department of Electrical Engineering, National Cheng Kung University, Tainan 701, Taiwan*
[b] *Center for Micro/Nano Science and Technology, National Cheng Kung University, Tainan 701, Taiwan*
[c] *Department of Electrical Engineering, Chienkuo Technology University, Changhua 500, Taiwan*

Received 16 August 2006; received in revised form 14 February 2007; accepted 23 February 2007
Available online 23 April 2007

**Abstract**

Lead-free $(Na_{0.5}K_{0.5})NbO_3$ ceramics doped with $CaTiO_3$ (0–3 mol%) have been prepared by the conventional mixed oxide method in this paper. All of the $CaTiO_3$ doped $(Na_{0.5}K_{0.5})NbO_3$ specimens do not deliquesce as exposed to water for a long time. The samples are characterized by X-ray diffraction analysis, Raman scattering spectra, scanning electron microscopy, and atomic force microscopy. The dielectric, piezoelectric and ferroelectric properties are also investigated. The results show that the addition of $CaTiO_3$ is very effective in preventing the deliquescence and in improving the electric properties of $(Na_{0.5}K_{0.5})NbO_3$ ceramics. Finally, surface acoustic wave devices based on lead-free ceramics have been successfully fabricated and their characterization is presented.


*Keywords:* Sintering; Piezoelectric properties; Niobates; Perovskites; $CaTiO_3$

## 1. Introduction

Single crystals and thin films for piezoelectric applications are mostly produced by special techniques, requiring increased process optimization and high cost. Modified ceramics have good potential due to their lower processing cost and ability to facilitate a desirable combination of properties, such as high surface phase velocity, electromechanical coupling coefficient ($k^2$) and low temperature coefficient of frequency (TCF). Lead oxide (PbO) based ceramics have been widely investigated and used for transducers, piezoelectric actuators, surface acoustic wave (SAW) filters and sensors because of their excellent piezoelectric properties.[1] We have reported many researches about modified lead titanate (PT) and lead zirconate titanate (PZT) ceramics used for SAW applications.[2,3] However, high volatilization of PbO may drive non-stoichiometry during firing process and its toxicity can contaminate the environment and damage human health. With the raise of environmental consciousness, therefore, it is the present tendency to develop excellent lead-free materials replacing Pb-based piezoelectric ceramics.

Sodium potassium niobate ($(Na_yK_{1-y})NbO_3$, NKN) ceramic is an attractive material and has been thoroughly investigated as a result of its high $k^2$ and high phase transition temperature ($T_c$ ~420 °C), especially near the morphotropic phase boundary (MPB).[4–6] Nevertheless, dense NKN ceramics are difficultly obtained since their phase stability is limited to 1140 °C.[7] Moreover, they would deliquesce once exposed to humidity due to the formation of extra phases.[6,7] The main problem is the volatilization of potassium oxide ($K_2O$) at 800 °C making the stoichiometry difficult to control.[7,8] Oxygen deficiency has been another problem in the preparation, which results from high-temperature processing and gives rise to electronic conductivity.[8] Many researchers used hot pressing or spark plasma sintering (SPS) techniques to yield better quality ceramics.[9] Recently, an efficient solution to improve foregoing problems is realized by utilizing some additives in NKN ceramics, such as $Pb_3O_4$, $PbTiO_3$, ZnO, $SrTiO_3$ (ST), $BaTiO_3$, $LiNbO_3$, $LiTaO_3$, etc.[7,10–17] The comparison of properties of

* Corresponding author at: Department of Electrical Engineering, National Cheng Kung University, Tainan 701, Taiwan. Tel.: +886 6 2757575x62381; fax: +886 6 2345482.
*E-mail address:* chusy@mail.ncku.edu.tw (S.-Y. Chu).

0955-2219/$ – see front matter © 2007 Elsevier Ltd. All rights reserved.
doi:10.1016/j.jeurceramsoc.2007.02.218

NKN ceramics based on the previous reports of various groups are demonstrated in Table 1. Furthermore, several groups have studied the effects of 0.5 mol% alkaline-earth (AE) dopant ($Mg^{2+}$, $Ca^{2+}$, $Sr^{2+}$, $Ba^{2+}$) and 0.5 mol% $AETiO_3$ on the properties of NKN-based ceramics.[18,19] It has been indicated that $CaTiO_3$ doping can promote densification of NKN ceramics and improve their properties.[18]

At present, the aim of this work is not only to synthesize $(Na_{0.5}K_{0.5})NbO_3$–$CaTiO_3$ (NKN–CT) ceramics by the conventional mixed oxide method and investigate their properties, but also to fabricate surface acoustic wave (SAW) devices further.

## 2. Experimental

The raw materials of $[(Na_{0.5}K_{0.5})_{1-x}Ca_x](Nb_{1-x}Ti_x)O_3$ samples ($NKN_{1-x}CT_x$), where $x = 0$–3 mol%, processed by a conventional mixed oxide method were pure reagent $Na_2CO_3$, $K_2CO_3$, $Nb_2O_5$, $CaCO_3$ and $TiO_2$ powders (>99.0% purity). First, 50 g of $Na_2CO_3$, $K_2CO_3$ and $Nb_2O_5$ powders were ball-milled in a 1000 mL polyethylene jar for 12 h with 400 g of 10 mm diameter $ZrO_2$ balls using 350 mL of ethanol (99.5% purity) as medium. The same procedure was applied to ball mill $CaCO_3$ and $TiO_2$ powders. Then, these slurries were separately dried and calcined at 950 °C in air for 10 h, respectively. After pulverization, the two powder batches were weighed according to the stoichiometric formula and ball-milled together. The resulting slurry was then dried, calcined and pulverized sequentially. These powders, milled with 8 wt.% PVA aqueous solution (5%), were uni-axially pressed into a disk of 12 mm diameter, at pressure of 25 kg/cm$^2$ and subsequently sintered in air at 1040–1120 °C, depending on the $CaTiO_3$ contents. A $K_2O$-rich atmosphere was maintained with NKN–CT powder to minimize the potassium loss during sintering process.

Bulk densities were measured by the Archimedes method using distilled water as medium. The crystallographic study was confirmed by X-ray diffraction (XRD) using Cu Kα ($\lambda = 0.154$ nm) radiation with a Seimens D-5000 diffractometer operated at 40 kV and 40 mA. The Raman scattering spectra excited by the 532.25 nm radiation were obtained with a micro-Raman spectrometer (Jobin Yvon, Labram HR) in the 200–1000 cm$^{-1}$ range at room temperature. The microstructure was observed by field emission scanning electron microscopy (FESEM) with a Hitachi S-4100 microscope. The dielectric (measured from 60 to 510 °C at 10 kHz) and piezoelectric properties were measured with a HP 4294A precision impedance analyzer. To measure the electrical properties, silver paste was painted on both sides of the samples to form electrodes, and then subsequently fired at 120 °C for 10 min. After that, samples were poled under 40 kV/cm DC field at 150 °C in a silicone oil bath for 30 min. The electromechanical coupling factor in thickness ($k_t$) and planar ($k_p$) mode was calculated from the resonance–antiresonance method. Ferroelectric hystersis loops ($P$–$E$) were obtained under 50 kV/cm ac field at 60 Hz by a modified Sawyer–Tower circuit.[20] The samples were also submerged in 150 °C silicon oil to prevent arcing.

In order to fabricate the SAW devices, the pellets were polished to a mirror finish on one side. Then, the interdigital

Table 1
Comparison of properties of $Na_{0.5}K_{0.5}NbO_3$ ceramics based on the previous reports of various groups

| Ceramic composition | $\rho$ (g/cm$^3$) | $\rho_r$ (%) | $\varepsilon'$ | $\varepsilon''$ (%) | $k_t$ (%) | $k_p$ (%) | $d_{33}$ (pC/N) | $N_t$ (kHz-mm) | $N_p$ (kHz-mm) | $Q_m$ | $TCF_B$ (ppm/°C) | $E_c$ (kV/cm) | $P_r$ (μC/cm$^2$) | Reference |
|---|---|---|---|---|---|---|---|---|---|---|---|---|---|---|
| NKN (hot pressed) | 4.46 | 98.9 | – | – | – | 45 | 160 | – | – | 240 | – | – | 33 | 6,7 |
| NKN | 4.25 | 94.2 | 290 | – | – | 36 | 80 | – | – | 130 | – | – | – | 6,12 |
| NKN | 4.3 | 95.3 | 472 | – | 45 | 39 | 110 | – | – | – | – | 20 | 20 | 6 |
| NKN–ZnO | ~4.26 | 94.5 | 500 | – | – | 40 | 123 | – | – | ~200 | – | 12 | 16 | 12 |
| NKN–$SrTiO_3$ | 4.44 | 98.4 | 412 | 4.0 | 43.8 | 32.5 | 96 | – | – | – | – | – | – | 7 |
| NKN–$BaTiO_3$ | 4.44 | 98.4 | – | 3.9 | 38 | 29 | 104 | – | – | – | – | 12 | 7.5 | 15 |
| NKN–$LiNbO_3$ | 4.35 | 96.5 | – | – | 48 | 44 | 235 | – | – | – | – | – | – | 16 |
| NKN–$LiTaO_3$ | – | – | 570 | – | – | 36 | 200 | – | – | – | – | 12.5 | 9 | 17 |
| NKN–$CaTiO_3$ | 4.40 | 97.6 | 553 | 4.0 | 42.1 | 37.9 | 115 | 2618 | 3377 | 267 | −311 | 12.2 | 12.4 | Our sample |

transducer (IDT) electrodes, made of 150 nm aluminum by thermal evaporation method, were patterned onto the polished surface using the lift-off photolithographic process. The surface roughness of polished ceramics was examined by atomic force microscopy (AFM) with a NT-MDT P7LS microscope using the tapping mode. The device characterization was measured with a HP 8714ES network analyzer (Agilent Technologies, Palo Alto, CA).

## 3. Results and discussion

It is commonly known that adding AE to substitute the perovskite structure by creating A site vacancies in case of NKN leads to an increase in density due to enhancement of sintering mechanism.[18] Adding CT and ST to NKN also can promote densification.[19] Fig. 1 shows the bulk densities of $NKN_{1-x}CT_x$ ceramics and their relative densities. The bulk density at 0.5 mol% CT addition reaches up to 4.40 g/cm$^3$, where the theoretical density is 4.51 g/cm$^3$.[6] The densities of the rest of the doped ceramics are in the range of 4.33–4.38 g/cm$^3$, equivalent to the relative densities 96–97%. None of the doped samples exhibit deliquescence against water, indicating that the CT addition can reduce the formation of unstable secondary phases enhancing the stability.

The X-ray diffraction patterns of the $NKN_{1-x}CT_x$ ceramics are shown in Fig. 2. The XRD pattern of $CaTiO_3$ powder is also added for comparison. The NKN–CT ceramics are composed of orthorhombic NKN and cubic CT. The main identified phase matches the orthorhombic NKN with space group *Amm*2 at room temperature, and the results reveal that the orthorhombic perovskite structure is preserved, when $x$ is varied from 0 to 3%.[21] $2\theta$ values for the orientations as a function of CT dopant are listed in Table 2. As increasing the CT content, the peaks shift toward a higher angle because the host $Na^+$ (ionic radius 1.39 Å) and $K^+$ (1.64 Å) are replaced by doped $Ca^{2+}$ (0.99 Å) and $Nb^{5+}$ (0.64 Å) is replaced by $Ti^{4+}$ (0.61 Å), respectively.[13,22]

XRD confirms the macroscopic symmetry in long-range ordering and Raman spectroscopy is sensitive to non-uniform distortions of the crystal lattice in short-range ordering.[21] According to the literature, the vibrations of $NbO_6$ octahedra are made up of $1A_{1g}(\nu_1)+1E_g(\nu_2)+2F_{1u}(\nu_3,\nu_4)+F_{2g}(\nu_5)+F_{2u}(\nu_6)$ in this case, where $\nu$ means the frequency band and $A_{1g}$, $E_g$, $F_{1u}$, $F_{1u}$, $F_{2g}$, and $F_{2u}$ indicate six species of vibration modes).[21,23] Of these vibrations, $1A_{1g}(\nu_1)+1E_g(\nu_2)+1F_{1u}(\nu_3)$ are stretching and the rest are bending modes.[21] Fig. 3 shows the Raman spectra of $NKN_{1-x}CT_x$ ceramics measured at room temperature. $\nu_5$ (262 cm$^{-1}$) and $\nu_1$ (616 cm$^{-1}$) are detected as relatively strong scattering. As the CT content increasing, the peaks for $\nu_1$ shift to a higher frequency and the full-width at half-maximum

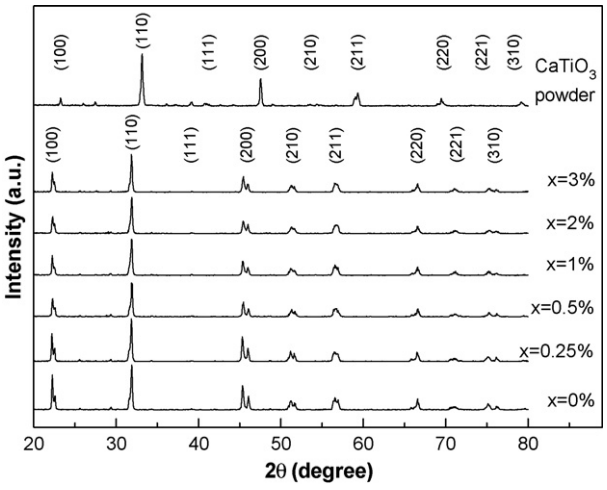


Fig. 2. X-ray diffraction patterns of the $NKN_{1-x}CT_x$ ceramics.

Table 2
$2\theta$ values for the orientations as a function of CT dopant

| CT dopant (mol%) | $2\theta$ value for the orientation (°) | | |
|---|---|---|---|
| | (1 0 0) | (1 1 0) | (2 0 0) |
| 0 | 22.250 | 31.885 | 45.362 |
| 0.25 | 22.242 | 31.873 | 45.345 |
| 0.5 | 22.268 | 31.908 | 45.395 |
| 1 | 22.275 | 31.891 | 45.406 |
| 2 | 22.279 | 31.894 | 45.438 |
| 3 | 22.277 | 31.896 | 45.450 |

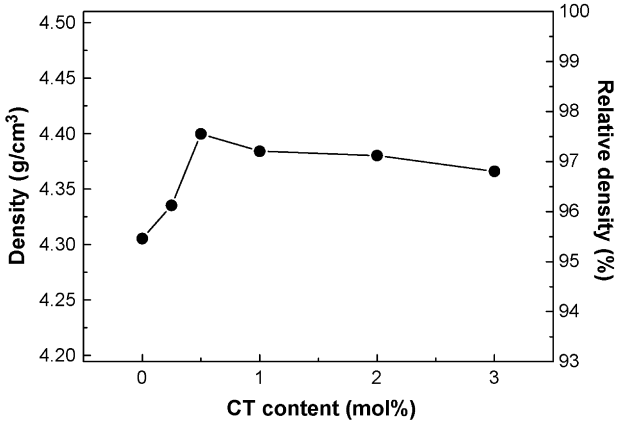


Fig. 1. The bulk densities of $NKN_{1-x}CT_x$ ceramics and their relative densities.

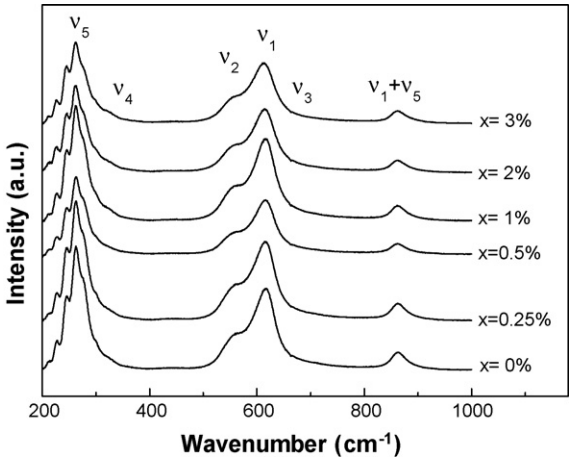


Fig. 3. Raman spectra of $NKN_{1-x}CT_x$ ceramics measured at room temperature.

(FWHM) also becomes broader. It is because of the incorporation of $CaTiO_3$ into the perovskite structure, which increases the binding strength of O–Nb–O.

Fig. 4 shows the SEM images and the grain size distributions of $NKN_{1-x}CT_x$ ceramics. It is distinctly observed that the grain size becomes smaller gradually with the increase of the CT content and thus, the doped ceramics are denser than the pure NKN. From the corresponding distributions of the grain size, it is very clear to note the increase in the number of small grains by adding CT.

Antiferroelectric $NaNbO_3$ possesses many phase transitions in wide temperature range (−100–643 °C). However, ferroelectric $KNbO_3$ combined with $NaNbO_3$ produces a new ferroelectric phase and displays three phase transitions around −120, 200 and 420 °C in the whole temperature range, corresponding to the transition temperatures of rhombohedral to

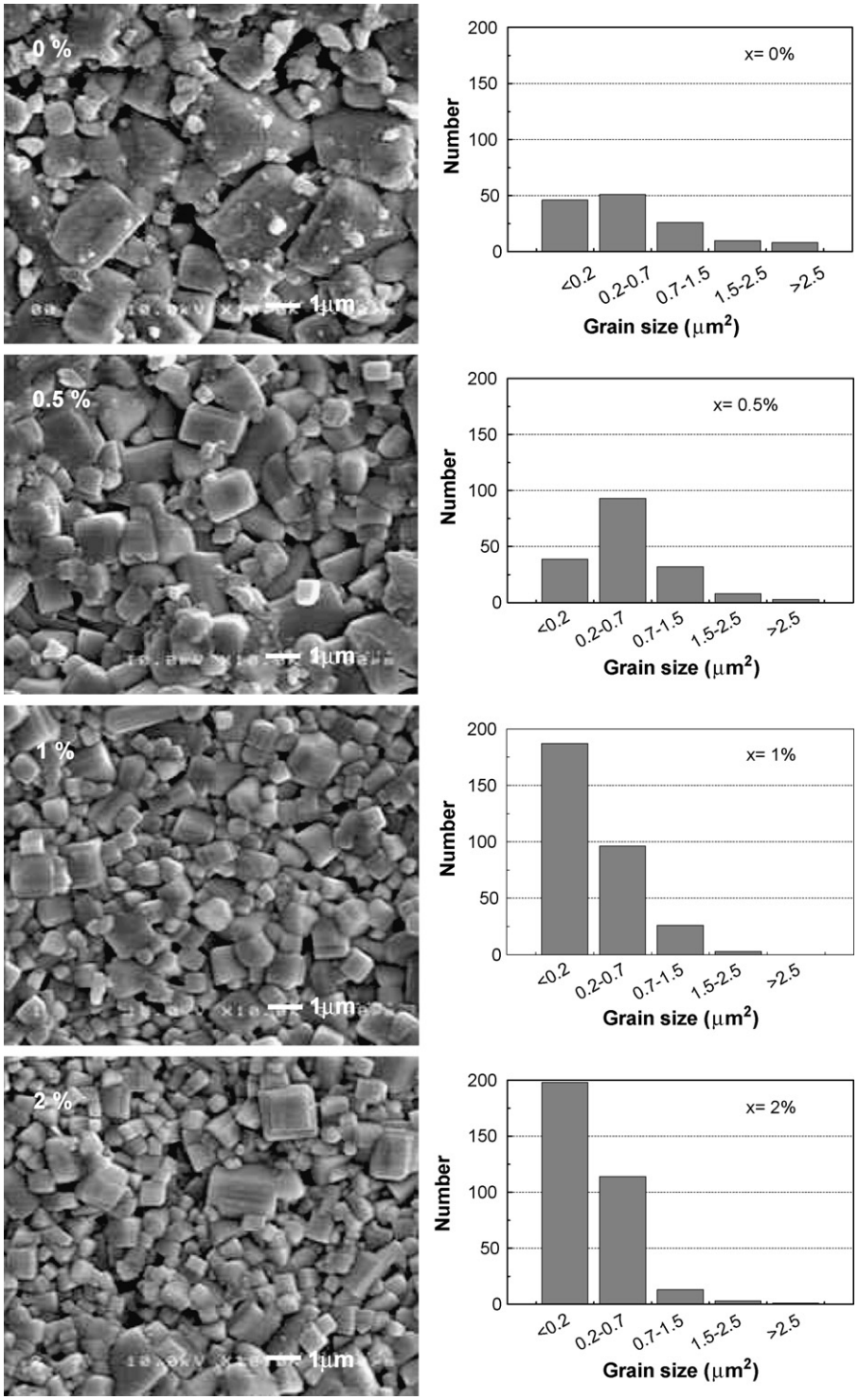


Fig. 4. The SEM images and the grain size distributions of $NKN_{1-x}CT_x$ ceramics.

orthorhombic, orthorhombic to tetragonal and tetragonal (ferroelectric) to cubic (paraelectric), respectively.[4,12,24] Fig. 5 shows the dielectric constant as a function of the temperature, and the dielectric constant and loss tangent versus CT content at room temperature. In Fig. 5(a), two-phase transitions are observed obviously above the room temperature and the peaks become broader as the increase of CT content. The two transition temperatures and the maximum value of dielectric constant at these temperatures also decrease with increasing CT additives. Previous investigations reported that the phenomenon has been found in many compounds,[7,13] such as (Pb,La)(Zr,Ti)$O_3$ and doped $BaTiO_3$. It is suggested that a transition from a normal ferroelectric to 'relaxor-like' ferroelectric due to the cation disorder in perovskite unit cell and the formation of microdomain since non-ferroelectric materials are added. In the experiment, the value of the Curie temperature for $CaTiO_3$ additive is found to be negative,[22] which exhibits quantum paraelectric phase at room temperature or higher. The relaxor behavior can be produced by many reasons.[7,13,14] In Fig. 5(b), the dielectric constant measured at room temperature and 10 kHz increases with increasing CT content, and the entire loss tangent of CT doped NKN is around 4%, which is less than pure NKN. Furthermore, according to the experimental results, the dielectric constant and loss tangent decrease with increasing the measuring frequency. Although their frequency dispersion both exist clearly between 1 and 10 kHz, the apparent higher

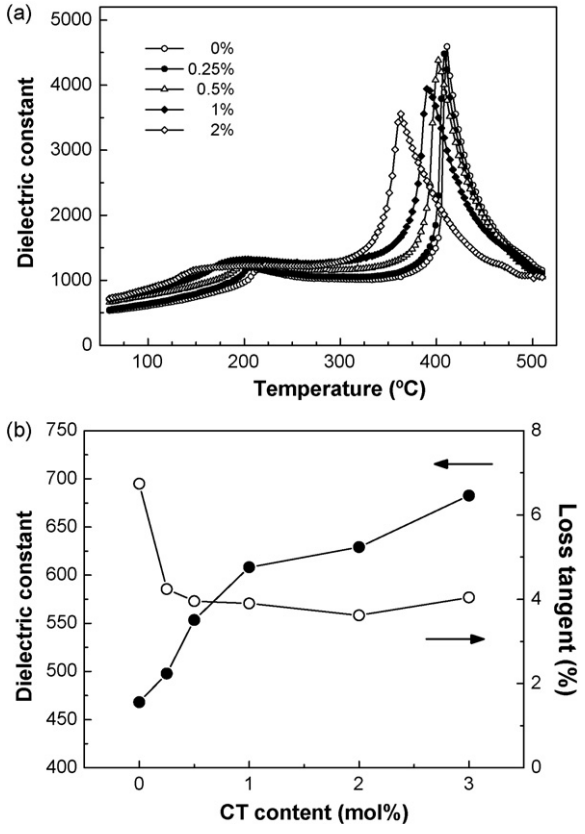


Fig. 5. (a) The dielectric constant as a function of the temperature for $NKN_{1-x}CT_x$ ceramics at 10 kHz and (b) the dielectric constant and loss tangent vs. CT content at room temperature.

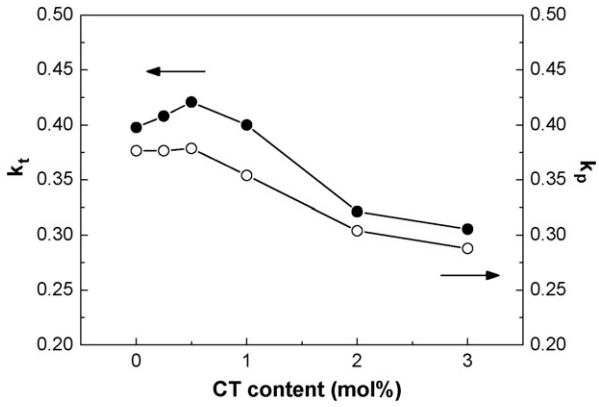


Fig. 6. Dependence of $k_t$ and $k_p$ of the NKN ceramics on the CT content.

frequency dispersion (10 kHz, 100 kHz, and 1 MHz) are not oberved.[19]

Dependence of $k_t$ and $k_p$ of the NKN ceramics on the CT content is shown in Fig. 6. CT doped ceramics (0.5 mol%) exhibit the maximum value of $k_t$ and $k_p$, reaching 42.1 and 37.9%, respectively. Addition of small amounts of CT yields to larger electromechanical coupling factors than those of pure NKN samples ($k_t = 39.8\%$ and $k_p = 37.6\%$). The promotion may be attributed to the increased density, lowering the leakage current and enhancing the poling process.[15] However, when the CT content exceeds 0.5 mol%, the values of $k_t$ and $k_p$ decrease gradually since the CT with a symmetry structure has no piezoelectricity. Other variations of piezoelectric properties are shown in Fig. 7, including the piezoelectric constant ($d_{33}$), the thickness frequency constant ($N_t$), planar frequency constant ($N_p$), mechanical quality factor ($Q_m$) and $TCF_B$ (the subscript "B" means bulk) values. The experimental results show that the NKN ceramics with 0.5 mol% CT provide the maximum values of $d_{33} = 115$, $N_t = 2618$ kHz-mm, $N_p = 3377$ kHz-mm and $Q_m = 267$. The ceramics with higher frequency constant can be used in higher frequency applications at identical bulk volume, and those with higher $Q_m$ provide reduced the mechanical loss. In addition, $TCF_B$ of all $NKN_{1-x}CT_x$ ceramics are negative and their absolute values increase correspondingly with increasing CT additive, which were determined from the shift of center frequency measurements at temperature from 25 to 80 °C, using the following equation:

$$TCF_B = \frac{f(80\,^\circ\mathrm{C}) - f(25\,^\circ\mathrm{C})}{(80-25)f(25\,^\circ\mathrm{C})}$$

Fig. 8 shows the ferroelectric properties of the $NKN_{1-x}CT_x$ ceramics measured at 150 °C and 60 Hz. The remanent polarization ($P_r$) is 15.7 μC/cm$^2$ and the coercive electric field ($E_c$) is 15.9 kV/cm for pure NKN ceramics. The $P_r$ and $E_c$ of 0.5 mol% CT content are 12.4 μC/cm$^2$ and 12.2 kV/cm, and those for 2 mol% CT are 8.4 μC/cm$^2$ and 10.1 kV/cm, respectively. With further increasing the doping content of CT, the values of $P_r$ and $E_c$ decrease. The results are shown in Fig. 8(b). The decrease in $P_r$ might be ascribed to the non-ferroelectric CT at room temperature, whereas, the decrease in $E_c$ is due to the increase of the bulk density that

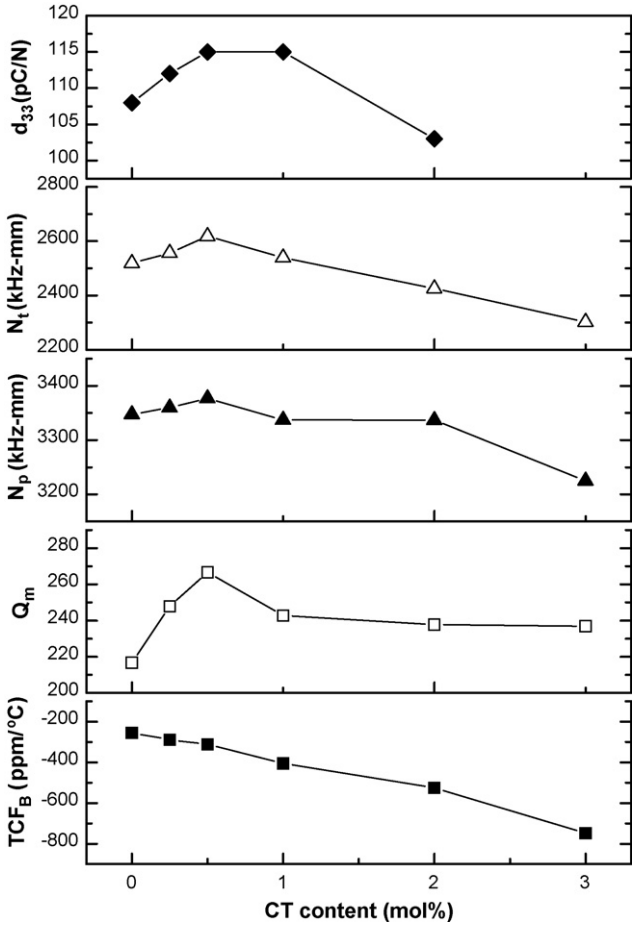


Fig. 7. Variations in $d_{33}$, $N_t$, $N_p$, $Q_m$ and $TCF_B$ values of the $NKN_{1-x}CT_x$ ceramics.

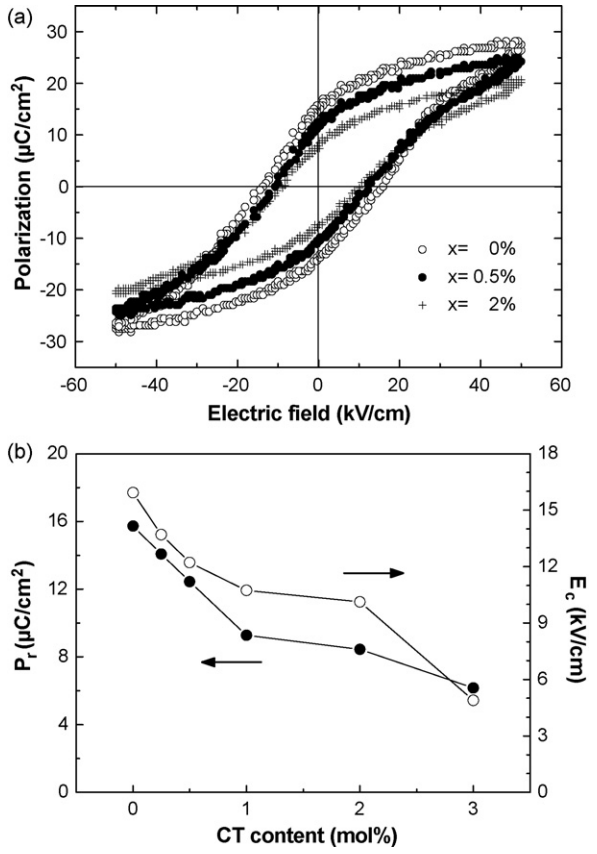


Fig. 8. (a) The $P$–$E$ hysteresis loops and (b) $P_r$ and $E_c$ variations of the $NKN_{1-x}CT_x$ ceramics measured at 150 °C and 60 Hz.

diminishes the leakage current enhancing the polarization in process.[12,15]

Surface acoustic wave can be generated at the free surface of an elastic solid. In the SAW devices, the generation of the waves is achieved by application of a voltage to a metal-film IDT deposited on the surface of a piezoelectric solid. Two IDTs are required in the basic SAW device. One of these acts as the device input and converts signal voltage variations into mechanical acoustic wave. The other IDT is employed as an output receiver to convert mechanical SAW vibrations back into output voltages. Such energy conversions require the IDTs to be used in conjunction with elastic surfaces that are also piezoelectric ones.[25] A SAW device configuration with IDTs/NKN–CT ceramic structure is shown in Fig. 9. IDT patterns were fabricated on the polished ceramic surface. The input and output IDTs consisted of 15.5 finger pairs with 20 μm width of electrode and 20 μm separation, i.e., a periodicity of 80 μm. The IDT center-to-center separation was 2.84 mm with a 4 mm aperture. Fig. 10 shows the frequency response of the SAW device for $NKN_{1-x}CT_x$ ceramics with $x = 0.5\%$. The center frequency of 40.475 MHz leads to a phase velocity of 3238 m/s, which is higher than many commercialized polycrystal-ceramics, for example, Pz27 (2016 m/s) and Pz34 (2510 m/s).[26] The insertion loss is quite large around 36.9 dB. One reason is owing to the rough surface probably. Fig. 11 shows the AFM images of $NKN_{0.995}CT_{0.005}$ ceramics with a polished surface. There are many cavities or voids on the surface. The root-mean-square roughness (Rq) without and with a polished surface are, respectively, 165.65 and 8.0 nm. The other reason may be due to itself

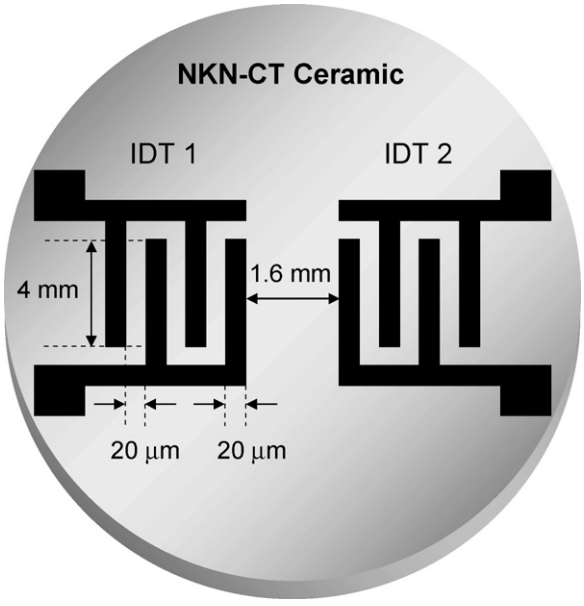


Fig. 9. A SAW device configuration with IDTs/NKN–CT ceramic structure.

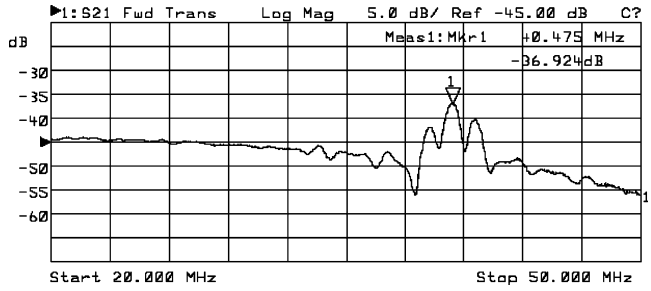


Fig. 10. The frequency response of the SAW device for $NKN_{1-x}CT_x$ ceramics with $x = 0.5\%$.

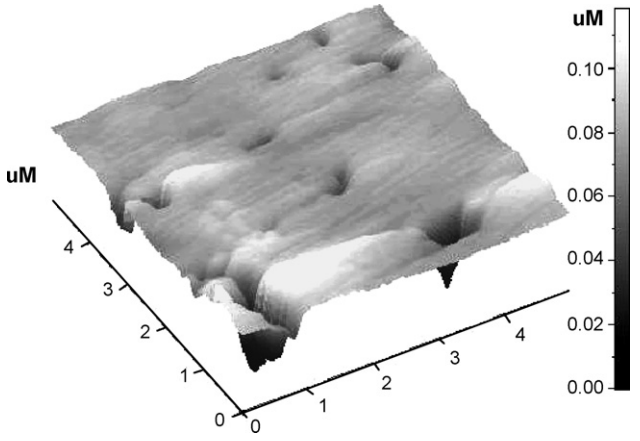


Fig. 11. The AFM images of $NKN_{0.995}CT_{0.005}$ ceramics with a polished surface.

characteristics. Moreover, it has high $k^2$ ~5.37% obtained from the equation[26]:

$$k^2 = \left(\frac{\pi}{4N}\frac{G_a}{B}\right)_{f=f_0}$$

where $N$ is the number of IDT fingers, and $G_a$ and $B$ are radiation resistance and susceptance, respectively. The $k^2$ is higher than most of PT-based ceramics (~1–4%).[26] Its $TCF_S$ (the subscript "S" means SAW) was calculated by substitution of center frequency for 0, 20, and 40 °C into the following equation:

$$TCF_S = \frac{f(40\,^\circ\mathrm{C}) - f(0\,^\circ\mathrm{C})}{(40-0)f(40\,^\circ\mathrm{C})}$$

Table 3
The parameters of NKN–CT ceramics and SAW device properties

| | |
|---|---|
| NKN–CT ceramic | |
| CT (mol%) | 0.5 |
| Sintering temperature (°C) | 1100 |
| Sintering time (h) | 3 |
| Poling filed (kV/cm) | 40 |
| Poling time (min) | 30 |
| SAW device | |
| $f$ (MHz) | 40.48 |
| $v$ (m/s) | 3238 |
| Insertion loss (dB) | −36.92 |
| $k^2$ (%) | 5.37 |
| $TCF_S$ (ppm/°C) | −292 |

The value arrives about −292 ppm/°C, which is higher than that of the SAW device based on single-piezocrystal substrate, such as LN128 (+75 ppm/°C), LN64 (−81 ppm/°C) and LT36 (−32 ppm/°C).[25] It is also much higher than Pb-based ceramic substrate (~−120–60 ppm/°C).[2,3,25,26] The parameters of NKN–CT ceramics and SAW device properties are listed in Table 3.

## 4. Conclusion

The properties of $NKN_{1-x}CT_x$ ceramics with $x = 0$–3 mol% by the conventional mixed oxide method have been investigated. None of the CT doped NKN specimens deliquesce as exposed to water for a long time. The dielectric constant at room temperature and the number of small grain sizes increases, and the transition temperatures decrease with increasing of CT content. CT doped NKN ceramics (0.5 mol%) show excellent piezoelectric properties of $k_t = 42.1\%$, $k_p = 37.9\%$, $d_{33} = 115$, $N_t = 2618$ kHz-mm, $N_p = 3377$ kHz-mm and $Q_m = 267$ which are better than pure NKN. However, the absolute values of the bulk TCF increase correspondingly with increasing CT additive. SAW devices based on $NKN_{1-x}CT_x$ ($x = 0.5$ mol%) ceramics have been successfully fabricated. The devices perform a phase velocity of 3238 m/s, high $k^2$ of 5.37%, and TCF about −292 ppm/°C. High $k^2$ and velocity make it possible to fabricate electromechanical transducers, however, it is unsuitable for applications on SAW filters ascribe to too large negative TCF. This unfavorable condition may have born fruitful results by doping or coating a thin film on it. As such, it might be promising for sensor applications because the high value of $k^2$ and velocity can enhance the sensitivity. Also the slight variation of temperature would be easily observed with high TCF value.

## Acknowledgements

This research was supported by the National Science Council (NSC) of Republic of China under grant NSC-95-2622-E-006-004-CC3. The authors also gratefully acknowledge the instrument assistance from Dr. Peng, Cheng-Jien in the Industrial Technology Research Institute (ITRI).

## References

1. Jaffe, B., Cook, W. R. and Jaffe, H., *Piezoelectirc Ceramics*. Academic, 1971, pp. 185–212.
2. Chu, S. Y. and Chen, T. Y., Fabrication of modified lead titanate piezoceramics with zero temperature coefficient and its application on SAW devices. *IEEE Trans. Ultrason. Ferroelectr. Freq. Control*, 2004, **51**, 663–667.
3. Chu, S. Y., Chen, T. Y., Tsai, I. T. and Water, W., Doping effects of Nb additives on the piezoelectric and dielectric properties of PZT ceramics and its application on SAW device. *Sens. Actuators A-Phys.*, 2004, **113**, 198–203.
4. Shirane, G., Newnham, R. and Pepinsky, R., Dielectric properties and phase transitions of $NaNbO_3$ and $(Na,K)NbO_3$. *Phys. Rev.*, 1954, **96**, 581–588.
5. Lingwal, V., Semwal, B. S. and Panwar, N. S., Dielectric properties of $Na_{1-x}K_xNbO_3$ in orthorhombic phase. *Bull. Mater. Sci.*, 2003, **26**, 619–625.
6. Birol, H., Damjanovic, D. and Setter, N., Preparation and characterization of $(K_{0.5}Na_{0.5})NbO_3$ ceramics. *J. Eur. Ceram. Soc.*, 2006, **26**, 861–866.
7. Guo, Y., Kakimoto, K. and Ohsato, H., Dielectric and piezoelectric properties of lead-free $(Na_{0.5}K_{0.5})NbO_3$–$SrTiO_3$ ceramics. *Solid State Commun.*, 2004, **129**, 279–284.

8. Chu, S. Y., Water, W., Juang, Y. D., Liaw, J. T. and Dai, S. B., Piezoelectric and dielectric characteristics of lithium potassium niobate ceramic system. *Ferroelectrics*, 2003, **297**, 11–17.
9. Matsubara, M., Yamaguchi, T., Kikuta, K. and Hirano, S., Effect of Li substitution on the piezoelectric properties of potassium sodium niobate ceramics. *Jpn. J. Appl. Phys.*, 2005, **44**, 6136–6142.
10. Tashiro, S., Nagamatsu, H. and Nagata, K., Sinterability and piezoelectric properties of $KNbO_3$ ceramics after substituting Pb and Na for K. *Jpn. J. Appl. Phys.*, 2002, **41**, 7113–7118.
11. Wang, R., Xie, R., Sekiya, T., Shimojo, Y., Akimune, Y., Hirosaki, N. *et al.*, Piezoelectric properties of spark-plasma-sintered $(Na_{0.5}K_{0.5})NbO_3$–$PbTiO_3$ ceramics. *Jpn. J. Appl. Phys.*, 2002, **41**, 7119–7122.
12. Park, S. H., Ahn, C. W., Nahm, S. and Song, J. S., Microstructure and piezoelectric properties of ZnO-added $(Na_{0.5}K_{0.5})NbO_3$ ceramics. *Jpn. J. Appl. Phys.*, 2004, **43**, L1072–L1074.
13. Kosec, M., Bobnar, V., Hrovat, M., Bernard, J., Malic, B. and Holc, J., New lead-free relaxors based on the $K_{0.5}Na_{0.5}NbO_3$–$SrTiO_3$ solid solution. *J. Mater. Res.*, 2004, **19**, 1849–1854.
14. Bobnar, V., Bernard, J. and Kosec, M., Relaxorlike dielectric properties and history-dependent effects in the lead-free $K_{0.5}Na_{0.5}NbO_3$–$SrTiO_3$ ceramic system. *Appl. Phys. Lett.*, 2004, **85**, 994–996.
15. Guo, Y., Kakimoto, K. and Ohsato, H., Structure and electrical properties of lead-free $(Na_{0.5}K_{0.5})NbO_3$–$BaTiO_3$ ceramics. *Jpn. J. Appl. Phys.*, 2004, **43**, 6662–6666.
16. Guo, Y., Kakimoto, K. and Ohsato, H., Phase transitional behavior and piezoelectric properties of $(Na_{0.5}K_{0.5})NbO_3$–$LiNbO_3$ ceramics. *Appl. Phys. Lett.*, 2004, **85**, 4121–4123.
17. Guo, Y., Kakimoto, K. and Ohsato, H., $(Na_{0.5}K_{0.5})NbO_3$–$LiTaO_3$ lead-free piezoelectric ceramics. *Mater. Lett.*, 2005, **59**, 241–244.
18. Malic, B., Bernard, J., Holc, J., Jenko, D. and Kosec, M., Alkaline-earth doping in $(K,Na)NbO_3$ based piezoceramics. *J. Eur. Ceram. Soc.*, 2005, **25**, 2707–2711.
19. Chang, Y., Yang, Z., Chao, X., Zhang, R. and Li, X., Dielectric and piezoelectric properties of alkaline-earth titanate doped $(K_{0.5}Na_{0.5})NbO_3$ ceramics. *Mater. Lett.*, 2007, **61**, 785–789.
20. Sawyer, C. B. and Tower, C. H., Rochelle salt as a dielectric. *Phys. Rev.*, 1930, **35**, 269–273.
21. Kakimoto, K., Akao, K., Guo, Y. and Ohsato, H., Raman scattering study of piezoelectric $(Na_{0.5}K_{0.5})NbO_3$–$LiNbO_3$ ceramics. *Jpn. J. Appl. Phys.*, 2005, **44**, 7064–7067.
22. Chandra, A., Ranjan, R., Singh, D. P., Khare, N. and Pandey, D., The effect of $Pb^{2+}$ substitution on the quantum paraelectric behaviour of $CaTiO_3$. *J. Phys.-Condens. Matter*, 2006, **18**, 2977–2994.
23. Last, J. T., Infrared-absorption studies on barium titanate and related materials. *Phys. Rev.*, 1957, **105**, 1740–1750.
24. Chu, S. Y., Water, W., Juang, Y. D., Liaw, J. T. and Dai, S. B., Properties of $(Na, K)NbO_3$ and $(Li, Na, K)NbO_3$ ceramic mixed systems. *Ferroelectrics*, 2003, **287**, 23–33.
25. Campbell, C. K., *Surface Acoustic Wave Devices for Mobile and Wireless Communications*. Academic Press, 1998, p. 20.
26. Chu, S. Y. and Chen, T. Y., The influence of Cd doping on the surface acoustic wave properties of Sm-modified $PbTiO_3$ ceramics. *J. Eur. Ceram. Soc.*, 2004, **24**, 1993–1998.